

A Cloudless Land Atmosphere Radiosounding database for generating Land Surface Temperature retrieval algorithms

J. M. Galve, C. Coll, V. Caselles, R. Niclòs, E. Valor, J.M. Sánchez, M. Mira
Department of Earth Physics and Thermodynamics, University of Valencia
46100, Burjassot, Valencia (SPAIN)
Joan.galve@uv.es

Abstract— A database of global, cloud-free, atmospheric radiosounding profiles was compiled with the aim of simulating radiometric measurements from satellite-borne sensors in the thermal infrared. The objective of the simulation is to generate split-window (SW) and dual-angle (DA) algorithms for the retrieval of land surface temperature (LST) from Terra/Moderate Resolution Imaging Spectroradiometer (MODIS) and Envisat/Advanced Along Track Scanning Radiometer (AATSR) data. The database contains 382 radiosonde profiles acquired over land, with nearly-uniform distribution of precipitable water between 0 and 5.5 cm. Radiative transfer calculations were performed with the MODTRAN 4 code. Different viewing angles were considered in the simulation, taking into account the features of each sensor. The viewing capability of AATSR, with near simultaneous observations first at a forward angle (55° from nadir) and then close to nadir, allows the implementation of DA algorithms. Using the simulation database, SW algorithms adapted for MODIS and AATSR data, and DA algorithms for AATSR data were developed. Both types of algorithms are quadratic in the brightness temperature difference, and depend explicitly on the land surface emissivity. A sensitivity analysis of all algorithms was made to obtain estimation of the algorithm errors. Furthermore the SW and DA algorithms developed from the simulation database were validated with actual ground measurements of LST collected, concurrently to MODIS and AATSR observations, in a site located close to the city of Valencia, Spain, in a large, flat and thermally homogeneous area of rice crops, where field campaigns were held during the summers of 2002-2006. Operational LST algorithms of each sensor were also validated in order to compare with the algorithms generated.

Keywords- Split-window, Dual angle, MODIS, AATSR, radiative transfer simulation, ground measurements

I. INTRODUCTION

Land Surface Temperature (LST) is a key magnitude in the study of energy and mass balance between surface and atmosphere. LST is needed as starting data in meteorological prediction models, evapotranspiration assessment, wildfire detection, and other applications. Moreover, it can be considered as an indicator of climatic global change and desertification processes. Thermal infrared remote sensing is the unique way to obtain this magnitude for large land extensions for different spatial resolutions and periodicities.

In order to obtain LST it is needed to correct the brightness temperature for atmospheric effects (absorption and emission mainly due to water vapor) and the surface emissivity effect. The drawback of this correction is the spatial and temporal variability of atmospheric water vapor and the dependence of the emissivity with land cover, structure and temporal evolution, for example.

The easiest, operational and most accurate correction methods are based on differential absorption in two observation conditions. If they are two different spectral bands in the atmospheric window between 10.5 μm and 12.5 μm the correction method is named Split-Window (SW). If the two conditions are two different observation angles, one at a large angle and the other close to nadir, the correction method is named Dual-Angle (DA). Usually, in both methods the LST is expressed as a linear or quadratic brightness temperature difference function, with constant coefficients having local or globally validity. These coefficients are obtained through radiometric measurements simulated for a set of atmospheric radiosoundings.

A new atmospheric radiosounding database is presented in this paper, CLAR (Cloudless Land Atmosphere Radiosounding). Through this database, and following the SW method proposed in [1], we obtained the coefficients needed for obtaining the LST from MODIS and AATSR data with different methods. MODIS bands 31 and 32 are suitable to use an SW method as well as AATSR bands at 11 and 12 μm . Moreover, the viewing capacity of AATSR, in which one target is observed firstly in forward view ($\sim 55^\circ$ from nadir) and 120 seconds after it is observed close to nadir ($< 23.5^\circ$ from nadir), allows the implementation of DA algorithms. All these algorithms are validated in a site close to Valencia, Spain, described in [2] and [3]. Operational LST algorithms of each sensor are also validated in order to compare them with the algorithms generated.

II. ALGORITHMS DEVELOPMENT

A. CLAR database

The CLAR database was compiled through the radiosounding collected by Atmospheric Science Department, University of Wyoming, available via the web page (<http://weatheruwyo.edu/upperair/sounding.html>). It contains a total of 382 radiosoundings taken in land meteorological stations

uniformly distributed. All the radiosoundings were taken from 2003 until 2006, and were checked by means of a cloud test in order to be sure that no cloud was included. A radiosounding was considered cloudy when one layer had relative humidity (RH) larger than 90 % or two consecutive layers had RH > 85 %. A radiosounding was considered foggy, and then rejected, when it had RH > 80% within the 2 first kilometres. CLAR has a good distribution in column water vapor content (W) which is uniform up to 5.5 cm and arrives up to close to 7 cm. It also has a good distribution between low, middle and high latitudes (40%, 40% and 20% respectively). The first layer temperature (T_0) ranges from -20 °C to 40 °C. The CLAR data base is available upon request to the authors.

B. Simulation characteristics

The algorithms generated were based on SW model of Coll and Caselles (1997). In this model the LST, T , can be expressed as :

$$T = T_1 + a_0 + a_1(T_1 - T_2) + a_2(T_1 - T_2)^2 + \alpha(1 - \varepsilon) - \beta \Delta \varepsilon \quad (1)$$

where T_i is the brightness temperature in condition i ($i=1$, 11 μm channel or nadir view; $i=2$, 12 μm channel or forward view), a_k are the atmospheric coefficients which only depend on atmospheric conditions, and α and β are the emissivity coefficients and can be expressed as a quadratic and linear function of column water vapor content, W . Theoretical expressions of these coefficients can be found in [1]. Finally ε and $\Delta \varepsilon$ are, respectively, the mean emissivity and emissivity difference between the two conditions considered. Since a_k are emissivity independent, they can be obtained via statistic regressions through brightness temperature simulations assuming a black body surface. Later and following [1], we can obtain α and β coefficients. The radiance measured with a sensor in the band i with at surface observation angle θ from nadir, $L_i(\theta)$, can be simulated from radiance emitted by the surface at temperature T according to :

$$L_i(\theta) = \tau_i(\theta) B_i(T) + L_i^\uparrow(\theta) \quad (2)$$

where B_i is the Planck function, $\tau_i(\theta)$ and $L_i^\uparrow(\theta)$ are the atmospheric transmittance and upward radiance, respectively. These are simulated using the multilayer radiative transfer model MODTRAN 4 [4]. The brightness temperature for channel i is obtained from the at sensor radiance, $L_i(\theta)$, following $B_i(T_i) = L_i(\theta)$. Each radiosounding of CLAR database was introduced in MODTRAN 4, in 65 layers from ground level to 100 km of altitude. Ground temperature, T , was taken depending on first layer temperature of each radiosounding, T_0 . Seven different temperatures were considered: $T_0 - 6^\circ\text{C}$, $T_0 - 2^\circ\text{C}$, $T_0 + 1^\circ\text{C}$, $T_0 + 3^\circ\text{C}$, $T_0 + 5^\circ\text{C}$, $T_0 + 8^\circ\text{C}$ y $T_0 + 12^\circ\text{C}$. Besides, six different at surface observation angles were considered, these angles are the Gaussian angles (11.6°, 26.1°, 40.3° and 53.7°), plus nadir and 65° for completeness.

III. LST ALGORITHMS

A. Algorithms developed

Four different algorithms were generated for AATSR, two SW algorithms and two DA algorithms. One SW is performed

for the nadir view, ASW_n , and the other for the forward view, ASW_f . ASW_n , is generated from simulations at the observation angles: 0°, 11.6° and 26.1°. ASW_f is generated from simulations obtained only for 53.7°. The two AATSR DA algorithms are generated from simulations obtained for two pairs of observation angles: 0°-53.7° and 11.6°-53.7°, in the AATSR channels at 11 μm (ADA11) and 12 μm (ADA12).

The algorithm for MODIS, MSW, was generated from simulations obtained for the observation angles: 0°, 11.6°, 26.1° and 40.3°. Since there are few studies about the angular variability of the emissivity, and due to the great degradation of regression results when angles larger than 45° are used, in this paper we restricted ourselves to $\theta < 45^\circ$. It should be noted that, for ASW_n and MSW , W is considered as the path column water vapor content, i.e. $W = W_0 / \cos \theta$, where W_0 is the vertical column water vapor.

The obtention of the atmospheric correction coefficients (a_0 , a_1 and a_2) is illustrated in Figure 1, which plots the differences $LST - T_1$ versus the brightness temperature differences ($T_1 - T_2$) for the MSW case. Atmospheric coefficients with their errors, adjustment error (σ_{AC}) and correlation coefficients (R^2) are shown in Table I.

Figure 2 plots the values of α and β coefficients versus W for the atmospheric profiles and surface temperatures of the CLAR database. The coefficients α and β can be expressed as:

$$\alpha = \alpha_0 + \alpha_1 W + \alpha_2 W^2 \quad (3)$$

$$\beta = \beta_0 + \beta_1 W \quad (4)$$

α_i and β_i coefficients are presented with their errors, $\sigma_{\alpha, \beta}$ and R^2 in Table II.

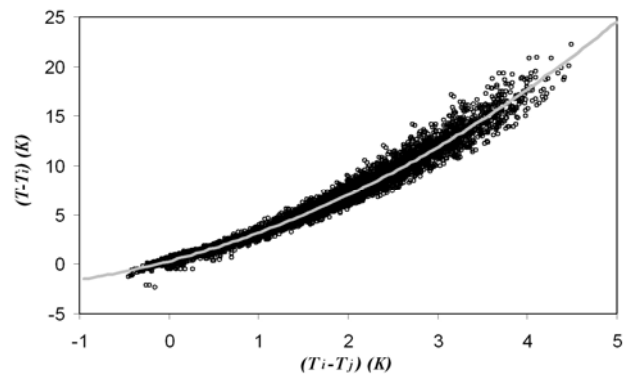


Figure 1. Static regression of $T - T_1$ versus the brightness temperature differences ($T_1 - T_2$) for obtaining the atmospheric coefficients. The MSW case is presented

TABLE I. ATMOSPHERIC COEFFICIENTS WITH THEIR STATICAL ERRORS FOR ALL ALGORITHMS

	ASW _n	ASW _f	ADA11	ADA12	MSW
a_0 (K)	0.024±0.018	0.16±0.07	-0.059±0.012	-0.01±0.03	0.319±0.011
a_1	0.782±0.016	0.49±0.06	1.569±0.012	1.57±0.03	2.370±0.017
a_2 (K ⁻¹)	0.320±0.03	0.437±0.007	0.176±0.002	0.303±0.005	0.494±0.005
σ_{AC} (K)	0.6	1.3	0.4	0.8	0.6
R^2	0.973	0.939	0.990	0.977	0.981

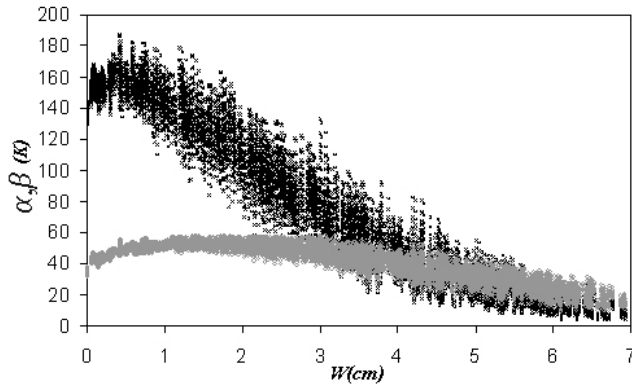


Figure 2. α (grey circle) and β (black cross) coefficient for MSW algorithm are represented in front of path water vapor content W (cm).

TABLE II. COEFFICIENTS FOR α AND β ESTIMATION

	ASWn	ASWf	ADA11	ADA12	MSW
α_0 (K)	52.57±0.14	55.2±0.3	57.00±0.17	64.5±0.2	45.99±0.13
α_1 (Kcm ⁻¹)	1.13±0.11	-4.4±0.2	1.57±0.12	-4.53±0.16	4.67±0.10
α_2 (Kcm ⁻²)	-1.023±0.017	-0.70±0.04	-1.18±0.02	-0.71±0.02	-1.446±0.014
σ_α (K)	5	6	4	5	5
R^2	0.979	0.959	0.985	0.978	0.974
β_0 (K)	79.2±0.2	64.6±0.4	111.6±0.3	110.3±0.4	160.5±0.3
β_1 (Kcm ⁻¹)	-11.06±0.06	-11.432±0.12	-17.62±0.07	-19.84±0.10	-25.75±0.08
σ_β (K)	9	11	9	13	15
R^2	0.837	0.805	0.928	0.896	0.916

B. Sensitivity analysis

Theoretical error, $\delta(T)$, was obtained as a combination of adjustment error, $\delta(\text{Coef.})$, of all the coefficients with the propagation of the error sources. The error sources are brightness temperatures, emissivity and W .

For the error in the brightness temperature, $\delta(T_i)$, we use the $NE\Delta T$ of both sensors which is 0.05 K ([6] and [7]). In order to estimate the final error associated to emissivity, $\delta(\varepsilon, \Delta\varepsilon)$, and considering that the variability of these parameters is the principal drawback to obtain LST we assume that typical error of the emissivity is 0.01. Vertical or path water vapor content has a typical error of 10% [8]. Table III presents the final error of the error source and the coefficient error adjustment. Finally, the last column shows the final theoretical error.

TABLE III. THEORETICAL ERRORS (K)

	$\delta(T_i)$	$\delta(W)$	$\delta(\varepsilon, \Delta\varepsilon)$	$\delta(\text{Coef.})$	$\delta(T)$
ASWn	0.2	0.06	0.8	0.6	1.1
ASWf	0.2	0.10	0.6	1.3	1.5
ADA11	0.2	0.07	1.0	0.4	1.1
ADA12	0.2	0.08	0.9	0.8	1.3
MSW	0.3	0.08	1.4	0.6	1.5

C. LST operational algorithms

The AATSR LST operational algorithm is implemented at the Rutherford Appleton Laboratory (RAL). This is based on the SW algorithm of [5] implemented with coefficients which depends on land cover type, i , precipitable water, p_w , fractional vegetation cover, f , and satellite zenith viewing angle, θ . RAL uses the coefficients from monthly $0.5^\circ \times 0.5^\circ$ lat/lon spatial resolution maps of i , f and p_w . LST images produced with this algorithm are currently provided with AATSR_L2 data.

The generalized SW LST operational algorithm of MODIS [9] uses coefficients obtained from linear regression of MODIS simulated data for wide range of surface and atmospheric conditions, and they depend on θ , W , the atmospheric lower boundary layer temperature. The LST product data can be obtained as MOD11 data.

IV. VALIDATION

For validating the algorithms developed and the LST operational algorithms we used a flat, large and thermally homogeneous area of rice crops located close to Valencia, Spain, where ground LST measurements were taken concurrently with MODIS and AATSR overpasses during summers of 2002-2006. The method to measure the ground LST and a study of the homogeneity of the site are presented in [2] and [3]. Mean emissivity and emissivity difference needed to apply our algorithms were measured using the box method [10] for AATSR channels. Then, in the case of ASWn we obtained $\varepsilon=0.983$ and $\Delta\varepsilon=0.005$ [3]. These values are only valid for nadir view. According to [3] a decrease around ~ 0.01 between nadir and forward view is assumed. Then we consider $\varepsilon = 0.973$ and $\Delta\varepsilon = 0.005$ for ASWf, $\varepsilon = 0.980$ and $\Delta\varepsilon = 0.010$ for ADA11 and $\varepsilon = 0.975$ and $\Delta\varepsilon = 0.010$ for ADA12. In the case of MSW, the emissivity is obtained through a 1 km² land cover classification [11]. Emissivity images can be obtained through MOD11 data. For the rice crop area, it yielded $\varepsilon = 0.983$ and $\Delta\varepsilon = -0.003$. Table 4 shows the statistics of the results for all algorithms. Though there are few points, Skewness and Kurtosis-3 factors are always less than unity which means that there is a good statistic.

ASWn and MSW have a RMSE less or equal to 1 °C. ASWf is the SW algorithm with largest RMSE (± 1.0 °C). This is because it has a large bias (0.6 °C) and standard deviation ($\sigma = \pm 0.8$ °C). The RMSE of DA algorithms is near ± 1.5 °C in all cases. They show an underestimation of LST close to 1.0 °C in all algorithms and a standard deviation larger than ± 1.0 °C. These errors make necessary further work in the study and characterization of the angular variation of emissivity.

The operational LST algorithm for MODIS show good results (RMSE= ± 0.6 K). The RAL algorithm shows an overestimation close to 3.5 K due to a non appropriate classification of our site. In fact, RAL classifies our site as broadleaf trees with ground cover with $f=0.45$. A better classification of our site is a full vegetation cover ($f=1$) of broadleaf shrubs with groundcover. The AATSR LST operational algorithm with this configuration can be expressed as:

$$T_{RAL2} = 0.4[\sec(\theta) - 1]p_w + 1.5662 + 3.1384(T_{11} - T_{12}) + 0.8965T_{12} \quad (5)$$

As shown in Table IV, both RAL and Eq (5) have the same standard deviation (*s.d.*) but the bias is reduced to close to zero with our classification.

V. SUMMARY AND CONCLUSIONS

The CLAR database was presented to generate LST retrieval algorithms for satellite sensor data. The radiosounding of CLAR are well distributed in *W* being uniform up to 5.5 cm. They also have a good distribution between low, middle and high latitudes (40%, 40% and 20% respectively). The first layer temperature T_0 ranges from -20 °C to 40 °C. Five different LST algorithms were generated with this database and using two different techniques: Split-Window (one for MODIS and two for AATSR) and Dual-Angle for AATSR.

TABLE IV. STATISTICS OF THE DIFFERENCES BETWEEN GROUND AND LSTS

	ASWn	ASWf	ADA11	ADA12	MSW	RAL	Eq.(5)	MOD11
Average \bar{X} (K)	0.0	0.6	-0.9	-1.0	0.0	-3.5	-0.1	0.1
s.d. (K)	0.5	0.8	1.1	1.2	0.4	0.6	0.6	0.6
RMSE (K)	0.5	1.0	1.5	1.6	0.4	3.6	0.5	0.6
Maximum difference (K)	1.1	2.4	1.4	1.5	1.1	-2.3	1.0	1.4
Minimum difference (K)	-1.0	-0.8	-3.2	-3.2	-0.5	-4.7	-1.0	-0.4
% cases in $\pm s.d.$	64	68	72	72	72.2	60	64	72
Skewness factor	0.2	0.4	0.3	0.2	0.97	0.06	0.14	1.3
Kurtosis-3 factor	-0.7	-0.3	-0.3	-0.4	0.03	-0.9	-0.4	0.2

The validation database of the Valencia test site was used to validate all these algorithms. The best results in terms of LST error were for ASWn (± 0.5 K) and MSW (± 0.4 K). These results confirm the conclusions shown in [2] and [3]. As shown in [3] Dual-Angle algorithms had an error close to ± 1.5 K. Reasons for this discrepancy could be errors in the angular variation of surface emissivity. In fact, as shown in the sensitivity analysis, the main error source in these algorithms is due to emissivity uncertainty. Moreover, the effect of the different spatial resolution between nadir and off-nadir views could be an important source of error.

Results of the validation of the operational LST products are equivalent to the results for the SW algorithms developed in this paper. The LST product offered by the RAL processor uses a too coarse spatial resolution. A more accurate spatial

resolution is needed for the classification of land surface. These results are in agreement with the conclusion presented in [2] and [3] with a more limited validation database.

ACKNOWLEDGMENT

Department of Atmospheric Science, University of Wyoming, is acknowledged for the atmospheric radiosoundings profiles. This work was financed by the Ministerio de Educación y Ciencia (project CGL2004-06099-C03-01, cofinanced with European Union FEDER funds, acciones complementarias CGL2005-24207-E y CGL2006-27067-E, and research grant of J.M. Galve). We thank the AATSR Validation Team, University of Leicester, European Space Agency (under CAT-1 project 3466) and EOS-NASA for providing the AATSR and MODIS data.

REFERENCES

- [1] C. Coll and V. Caselles, "A split-window algorithm for land surface temperature from Advance Very High Resolution Radiometer data: Validation and algorithm comparison", *Journal of Geophysical Research*, 102, 16697-16713, 1997.
- [2] Coll, C., Caselles, V., Galve, J.M., Valor, E., Niclòs, R., Sánchez, J.M. and Rivas R., "Ground measurements for the validation of land surface temperatures derived from AATSR and MODIS data", *Remote Sensing of Environment*, 97, 288-300, 2005.
- [3] Coll, C., Caselles, V., Galve, J.M., Valor, E., Niclòs, R., and Sánchez, J.M., "Evaluation of split-window and dual-angle correction methods for land surface temperature retrieval from Envisat/AATSR data". *Journal of Geophysical Research*, 111, 12105 doi 10.1029/2005JD006830, 2006.
- [4] Berk, A., Anderson, G.P., Acharya, P.K., Chetwynd, J.H., Bernstein, L.S., Shettle, E.P., Matthew, M.W., and Adler-Golden, J.H., "MODTRAN 4 users manual, report". Air Force Research Laboratory Space Vehicles Directorate, Hascom AFB, Mass, 1999.
- [5] Prata, A. J., "Land surface temperature measurement from space: AATSR algorithm theoretical basis document". *Technical report*, CSIRO. 2000, 27 pp.
- [6] Toller, G.N. and Isaacman, A., "MODIS Level 1B Product User's Guide", *NASA/Gooddard Space Flight Center*, Greenbelt, MD 20771, 2003.
- [7] AATSR Product Handbook, Issue 2.1, 28th of March of 2006, <http://envisat.esa.int/dataproducts/aatsr/>.
- [8] Seemann, S.W., Borbas E.E., Li J., Menzel, W.P. and Gumley L.E., "MODIS atmospheric profile retrieval Algorithm Theoretical Basis Document", 40pp, *Madison*, WI 53706, 2006.
- [9] Wan, Z. and Dozier, J., "A generalized split-window algorithm for retrieving land surface temperature from space", *IEEE Transactions on Geoscience and Remote Sensing*, 34, 892-905, 1996.
- [10] Rubio, E., Caselles, V., Coll, C., Valor, E., and Sospedra, F., "Thermal-infrared emissivities of natural surfaces: Improvements on the experimental set-up and new measurements". *International Journal of Remote Sensing*, 24(24), 5379- 5390, 2003.
- [11] Snyder, W.C. and Wan, Z., "BRDF to predict spectral reflectance and emissivity in the thermal infrared", *IEEE Transactions and Remote Sensing*, 36(1): 214-225, 1998.